

GeneGAN: Learning Object Transfiguration and Attribute Subspace from Unpaired Data

Shuchang Zhou¹
shuchang.zhou@gmail.com

Taihong Xiao^{1,2}
xiaotaihong@pku.edu.cn

Yi Yang¹
yangyi@megvii.com

Diejiao Feng¹
fdj@megvii.com

Qinyao He¹
hqy@megvii.com

Weiran He¹
myr@megvii.com

¹ Megvii Inc.
Beijing, China

² Department of Information Science,
School of Mathematical Sciences,
Peking University
Beijing, China

Abstract

Object Transfiguration replaces an object in an image with another object from a second image. For example it can perform tasks like “putting exactly those eyeglasses from image A on the nose of the person in image B”. Usage of exemplar images allows more precise specification of desired modifications and improves the diversity of conditional image generation. However, previous methods that rely on feature space operations, require paired data and/or appearance models for training or disentangling objects from background. In this work, we propose a model that can learn object transfiguration from two unpaired sets of images: one set containing images that “have” that kind of object, and the other set being the opposite, with the mild constraint that the objects be located approximately at the same place. For example, the training data can be one set of reference face images that have eyeglasses, and another set of images that have not, both of which spatially aligned by face landmarks. Despite the weak 0/1 labels, our model can learn an “eyeglasses” subspace that contain multiple representatives of different types of glasses. Consequently, we can perform fine-grained control of generated images, like swapping the glasses in two images by swapping the projected components in the “eyeglasses” subspace, to create novel images of people wearing eyeglasses.

Overall, our deterministic generative model learns disentangled attribute subspaces from weakly labeled data by adversarial training. Experiments on CelebA and Multi-PIE datasets validate the effectiveness of the proposed model on real world data, in generating images with specified eyeglasses, smiling, hair styles, and lighting conditions etc. The code is available online.

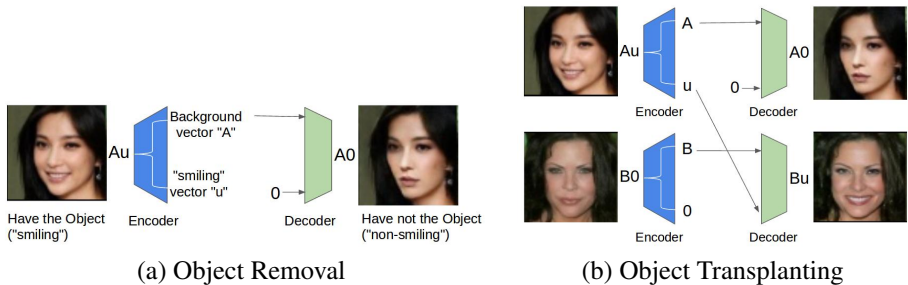


Figure 1: (a) Encoder of GeneGAN decomposes an image to the background feature A and the object feature u . The decoder can reconstruct an image without the object (a non-smiling face), from background feature A and the zero object feature (denoted as 0). (b) Decomposed object feature can be used to transplant the object to another image. When the “smiling” feature u , which is from the first image Au , and the background feature B are fed to a decoder, the generated image Bu would ideally have the same level and style of smiling as Au .

1 Introduction

Object transfiguration is a type of conditional image generation, that first decomposes an image into an object part and background part. The object is then modified to satisfy a particular condition, and the background is kept unchanged. Object transfiguration has found applications in image editing [0, 5, 13, 23, 27, 28], and image synthesizing [0, 13, 24]. Depending on the task, the object can be concrete instances like eyeglasses, or more abstract concepts like facial expressions. The generated images would then be answers to questions like “what if her eyeglasses is on my nose?” or “what if I smile like her?”

Under the Linear Feature Space conjecture [10] for features extracted by Deep Neural Networks, we may achieve complex object transfiguration tasks like removal and transplanting of objects, by linear operations on the feature vectors. The images generated from the modified feature vectors can still be natural-looking and has negligible artifacts. In fact, previous works [19, 23] have shown that making a face in an image smile, is as simple as addition with an vector in feature space:

$$\text{smiling face} = \phi^{-1}(\phi(\text{non-smiling face}) + \mathbf{v}_{\text{smiling}}), \quad (1)$$

where ϕ is a mapping from images to features, and the transform vector $\mathbf{v}_{\text{smiling}}$ can be computed as the difference between clustering centers of features of smiling faces and non-smiling faces.

However, there are many styles and levels of smiling. For example, some kinds of smiling do not expose teeth, and some are more manifested in eyes than in mouth. Hence representing smiling by a single transform vector will severely limit the diversity of smiling in generated images. To address this diversity issue, the Visual Analogy-Making [24] method proposes to use a pair of reference images to specify the transform vector, for example two images where the same person smiles in one and not in the other. Though this method increase the diversity, such paired data are hard to acquire except in controlled environments.

Yet another approach to Object Transfiguration is the recently proposed GAN with cyclic loss approach, which exploits Dual Learning [8, 11, 26, 29] to map between the source images (non-smiling faces) and the target images (smiling faces). Nevertheless, Dual Learning

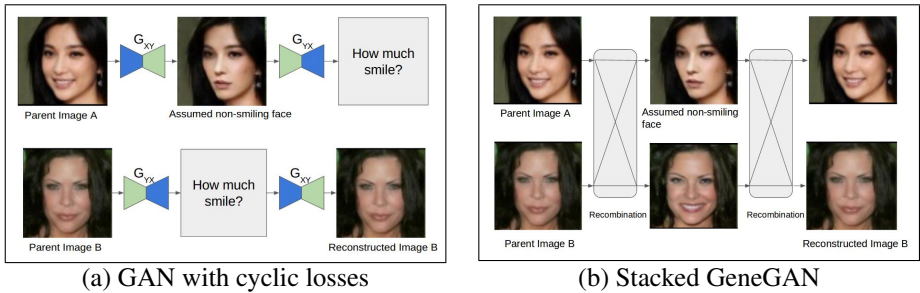


Figure 2: (a) The method of GAN with cyclic losses suffers from under-determination problem when removing an object: there will be incomplete information when going from non-smiling faces to smiling faces to determine the level and style of smiling in generated images. (b) The alternative Stacked GeneGAN model. The smiling of two images are swapped twice, through recombinations, to reconstruct the original images.

relies on the invertibility of the mapping for the cyclic loss to work. When the intrinsic dimension of the source and target domains are not the same, like when the source domain does not have the object and the target domain has it, the cyclic loss cannot be applied. More discussions will be left to Section 2.4.

In this work, we propose a model that can generate an object feature vector (hereafter shortened as “object feature” or “object vector”) from a single image. The object feature can then be transplanted to other images to generate novel images with similar objects. Our model is made up of two parts: an Encoder that decomposes an image to a background feature part and a object feature part, and a Decoder that can combine a background feature and an object feature to produce an image. Figure 1 illustrates typical usage patterns of the proposed model: object removal and object transplanting, which are both done by some wiring of Decoders and Encoders. All instances of Decoders and Encoders share parameters respectively.

Moreover, object features from the Decoder are found to constitute a vector space: the non-presence of objects is mapped to the origin, the norm is proportional to the strength of the object (like level of smiling), and linear combinations produce other feasible object features. Though previous works [19, 23] also observe that the one-dimensional attribute vector also demonstrates these properties, we are able to extract higher dimensional attribute subspace, due to the increasing of diversity of object features. Experiments on face attributes like hair styles and eyeglasses demonstrate the richness of such attribute subspaces. We perform experiments in a proprietary Deep Learning framework, and a Tensorflow implementation is available at <https://github.com/Prinsphield/GeneGAN>.

2 Method

In this section, we formally outline our method and present the problem of learning the disentangled representation for backgrounds and objects.

The training data is made of two sets: the set of image having the attributes is $\{x_{Au}^i\}_{i=1}^N$, and the opposite set being $\{x_{B0}^i\}_{i=1}^M$, where u and 0 stands for presence/non-presence of an object respectively. The two sets of images need not be paired. The division of training data into two sets is effectively a 0/1 labeling over all training data.

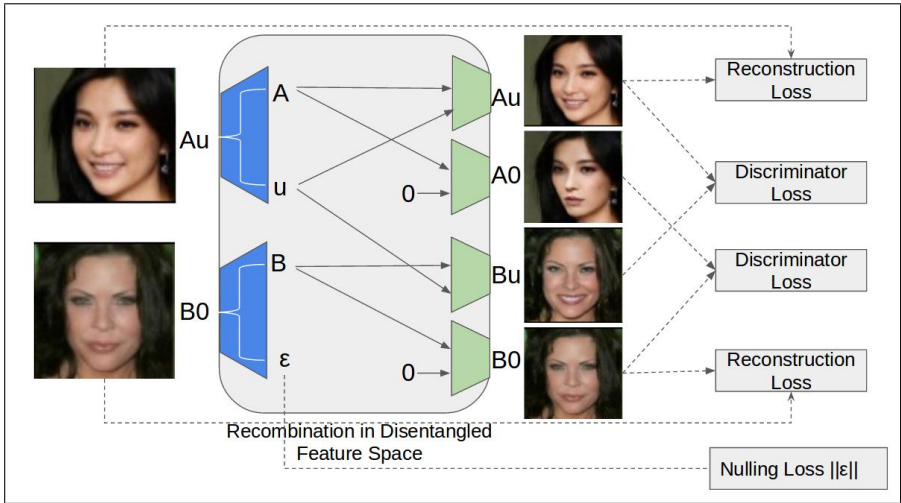


Figure 3: The training diagram of GeneGAN. The information about the smiling in image A_u is flowed to its reconstructed version and image B_u through object feature u .

2.1 Model

Our model is made up of an Encoder that maps an image to two complement codes, and a Decoder that is inverse of Encoder. Division of the codes is unknown have to be learned from the 0/1 labeling. To achieve the disentangling of object features from background features, we would like the following constraints to be satisfied:

1. An image without any objects should be indistinguishable from the set $\{x_{B_0}^i\}_{i=1}^M$.
2. An image that does have the object should be indistinguishable from the set $\{x_{A_u}^i\}_{i=1}^N$.

Here x_{A_u} stands for an image that will be decoded to A and u . We will sometimes refer to the image x_{A_u} simply as A_u when it is clear from context.

Such “indistinguishable” constraint can be enforced by introduction of adversarial discriminators [6, 7], which interprets indistinguishable as “there does not exist discriminator that can assigns different score to two sets”.

This inspires us to introduce the training diagram as illustrated in Figure 3 for our model, namely GeneGAN. During training, four children A_u , A_0 , B_u , B_0 are created out of combinations of complement codes of two parent images A_u and B_0 as follows: first, the Encoder will create four pieces of codes for the two images, namely A , u , B and 0 ; then Decoders will create four legal recombinations as children: A_u , A_0 , B_u , B_0 .

Out of four children, two recombinations A_u and B_0 are exact reconstructions, while A_0 and B_u are novel crossbreeds. By using an adversarial Discriminator to require that A_u being indistinguishable from B_u , and that we can reconstruct A_u from A and u , we can enforce all information about the object to be encoded in u . Similarly, if A_0 is not distinguishable from B_0 , we can ensure that A does not contain any information about the object. Overall, we can achieve the disentanglement of the object information from the background information.

Moreover, the reconstruction losses will induce u and v to contain the complete information about the object. Inclusion of reconstruction loss also stabilizes the training of Adversarial Discriminator [11, 26, 29].

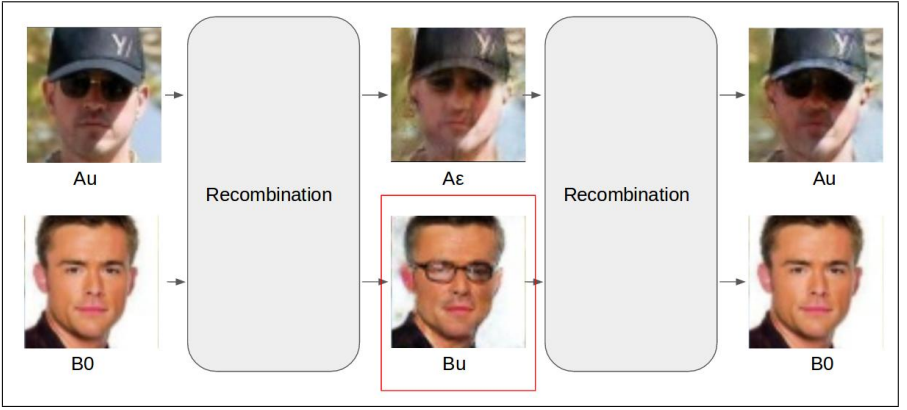


Figure 4: The objects in Au and Bu may have difference appearances.

2.2 Attribute Drift Problem and Parallelogram Constraint

Through experiments, sometimes we observe a problem of ‘‘Attribute Drift’’: the visual appearance of the objects may be different between Au and Bu , even though there will still be a one-to-one correspondence between the two objects. An illustrative example is given in Figure 4, when Au is a man wearing sunglasses with black lens and $B0$ is a man not wearing any eyeglasses. It is possible that Bu will be the second man wearing any kind of eyeglass, as long as there is still a one-to-one correspondence between the eyeglasses of Bu and eyeglasses of Au .

Instead of applying an additional classifier to enforce that styles of the objects of Au and Bu be the same, we propose the following parallelogram constraint on the image domain when objects are approximately aligned: the sum of image pixel values of Au and $B0$, should be approximately the same as the sum of $A0$ and Bu . In the above example, this will encourage a sun glass, when transplanted, to stay as a sun glass, and not mutating into an eyeglass.

Note it will not make sense to include the parallelogram loss for GAN with cyclic losses, as the transformation of two original images are completely independent of each other. In their case, adding a parallelogram loss will only increase the overfitting level of the model.

2.3 Loss Function of Training

Given two images x_{Au} and x_{B0} , the data flow of training of GeneGAN can be summarized in following equations:

$$\begin{aligned}
 (A, u) &= \text{Encoder}(x_{Au}) & (B, \varepsilon) &= \text{Encoder}(x_{B0}) \\
 x_{A0} &= \text{Decoder}(A, 0) & x_{Bu} &= \text{Decoder}(B, u) \\
 x'_{Au} &= \text{Decoder}(A, u) & x'_{B0} &= \text{Decoder}(B, 0)
 \end{aligned} \quad (2)$$

We force the ε encoded from $B0$ to be zero, so as to ensure the constraint that $A0$ should not contain any information about $B0$, and that any information contained in the object part of $B0$ can be safely discarded.

The generator receives four types of losses: (1) the standard GAN losses, which measures how realistic the generated images are; (2) the reconstruction losses, which measures how well the original input is reconstructed after a sequence of encoding and decoding. (3) the

nulling losses, which reflects how well the object features are disentangled from background features and (4) (optionally) the parallelogram losses, which enforces a constraint between the children and the parents in image pixel values. We omit the weights of the losses and left the details to online implementation. P_0 and $P_{\neq 0}$ stand for the distribution of images without and with the objects, respectively.

$$\begin{aligned}
 L_{reconstruct}^{Au} &= \|x_{Au} - x'_{Au}\|_1 & L_{reconstruct}^{B0} &= \|x_{B0} - x'_{B0}\|_1 \\
 L_{GAN}^0 &= -\mathbb{E}_{z \sim P_0} [\log D(x_{A0}, z)] & L_{GAN}^{\neq 0} &= -\mathbb{E}_{z \sim P_{\neq 0}} [\log D(x_{Bu}, z)] \\
 L_0 &= \|\varepsilon\|_1 & L_{parallelogram} &= \|x_{Au} + x_{B0} - x_{A0} - x_{Bu}\|_1 \\
 L_G &= L_{reconstruct}^{Au} + L_{reconstruct}^{B0} + L_{GAN}^0 + L_{GAN}^{\neq 0} + L_0 + L_{parallelogram}
 \end{aligned} \tag{3}$$

The nulling loss will push the background information to the B part. In fact, the object output of encoder will not contain background information, as ε is forced to zero.

The Reconstruction losses will serve multiple purposes. First, the reconstruction losses associated with Au and $B0$ will ensure that Decoder and Encoder are inverse to each other. In addition, A is forced to contain background information, to allow Decoder to reconstruct Au from A and u .

The discriminator receives the standard GAN discriminator loss

$$\begin{aligned}
 L_D^0 &= -\mathbb{E}_{z \sim P_0} [\log D(x_{Au}, z)] - \mathbb{E}_{z \sim P_0} [\log(1 - D(x_{Bu}, z))] \\
 L_D^{\neq 0} &= -\mathbb{E}_{z \sim P_{\neq 0}} [\log D(x_{A0}, z)] - \mathbb{E}_{z \sim P_{\neq 0}} [\log(1 - D(x_{B0}, z))] \\
 L_D &= L_D^0 + L_D^{\neq 0}
 \end{aligned} \tag{4}$$

The Discriminator losses will ensure the recombinations be of desired property.

As we enforce constraints by losses, the constraints hold only approximately and there will be potential leakage of information between the object and feature parts. We leave it as future work to explore even stronger enforcement of constraints.

2.4 Alternative Stacked GeneGAN

Method of GAN with cyclic loss suffers from under-determination problem when performing object removal and reconstruction. For example, in Figure 2(a), though the non-smiling version of a smiling face is well defined, it is hard to determine how much smiling should be present when mapping from the non-smiling faces to smiling faces.

However, it is also possible to add cross-links to allow communication of information. In fact, we have also experimented with a training diagram closer to the method of GAN with cyclic losses, as illustrated in Figure 2. The difference between this and Figure 3 is that only crossbreeds are created as children of the parent images. The children will be recombined again to produce grand-children, which ideally have the same features as their grand-parents. Reconstruction losses can then be used to enforce this invariance, exactly as is done in the method of GAN with cyclic losses.

However, we find this ‘‘double-swap’’ training diagram to be inferior in experiments. We observe that the reconstruction losses will be significantly higher as the grand-children went through more nonlinear transformations. We conjecture that the higher reconstruction losses will compete more with the adversarial losses, and create instability of training and degrades the quality of generated images.

3 Experiments

In this section we perform experiments on real-world datasets to validate the effectiveness of our method. For training, we used learning rate of $5e-5$ and momentum of 0, under RMSProp [12] learning rule. The Neural Network models used in this section are all equipped with Batch Normalization [10] to speedup convergence. The encoders have three layers of convolutions with Leaky ReLU nonlinearity [16]. The decoders have three convolution layers with fractional stride [12]. More details of the models will be available online.

Experiments are done on Linux machines with Intel Xeon CPUs and NVidia TitanX Graphic Processing Units.

3.1 Dataset

The CelebA [14] dataset is a large-scale face attributes dataset including 202599 face images of 10177 identities, each with 40 attributes annotations and 5 landmark locations. The landmark locations can be used to spatially align the faces.

The Multi-PIE database [15] contains over 754,200 images from 337 subjects, captured under 15 viewpoints and 19 illumination conditions.

3.2 Swapping of Attributes

As GeneGAN only exploits the weak 0/1 labels of the images, and that there will be no training data about the recombined versions, we will not distinguish between the training data and test data in experiments carried out in this subsection.

An object can be removed by passing in ϵ to the Decoder. Similarly, an object can be replace by replacing the object input to the decoder. As our model can disentangle the object part from background part, the crossing usage pattern as illustrated in Figure 1(b) can also be used to swap the attributes.

In each row of the following diagram, the object parts of the images are overridden by the objects of the first image in the row. Of particular interest is Figure 5(a). It can be observed that the hair styles follow closely the source images on the top row. In fact, the directions of hairs is in good agreement with the source images.

3.3 Generalization to Unseen Images and Comparisons with GAN with cyclic losses

Figure 7 compares GeneGAN with DiscoGAN. Though DiscoGAN may also reconstruct images that are of good quality, the objects in the reconstructed images are not quite related to the original images. In contrast, GeneGAN produces consistent reconstruction.

Figure 8 gives results of testing a GeneGAN model trained on CelebA dataset on the Wider Face dataset, which contains face images in even less constrained environments. It can be seen that the GeneGAN model generalizes well to unseen data.

3.4 Interpolation in Attribute Subspace

Figure 9 gives interpolation of object features in attribute subspace. Note the backgrounds (human identities) are approximately the same, while objects (hair styles) are interpolated.



(a) hair style



(b) smiling



(c) glasses

Figure 5: Replacing the object for images in each row with those of the column heads.



Figure 6: Swapping the lighting conditions of two faces on Multi-PIE dataset. From left to right, the six images in a row are: original Au and BE , recombined AE and Bu , and reconstructed Au and BE respectively.



(a) GAN with cyclic losses

(b) GeneGAN

Figure 7: Comparison between GAN with cyclic losses (the best model before divergence), and GeneGAN. The top row, middle row, and the bottom row are images with original, removed and reconstructed objects respectively.



Figure 8: Performance of GeneGAN on unseen data from Wider Face [25].



Figure 9: The attribute space as interpolated by several object feature vectors.

4 Related Work

In this section we discuss related work not yet covered.

Using autoencoders for transforming images may be traced back to Hinton *et al.* [9]. When one of the disentangled space is known, like having class labels, techniques like statistical independence can be used to disentangle the two spaces [6, 12, 15, 20]. In this work, we do not assume that any of the two spaces have additional supervision signals.

5 Conclusion

This paper presents GeneGAN, a deterministic conditional generative model that can perform object transfiguration task, which is modification of an object in an image with background unchanged. The proposed model learns to disentangle the object features from other factors in feature space from weakly supervised 0/1 labeling of training data. Consequently, our model can extract an object feature vector from a single image and transplanted it to another image, hence allows fine-grained control of generated images, like “putting eyeglasses of A onto noses of B”. The objects can be abstract and difficult to characterize, like hair styles and lighting conditions. The training method for our model is symmetric and allows exploiting cyclic reconstruction loss, which improves stability of training.

The setup of our model also gives rise to an attribute subspace, which contains multiple vectors that are representatives of different objects. The vectors can be scaled, inverted and interpolated to manipulate the objects in generated images.

As future work, it would be interesting to investigate whether more complex crossbreeding patterns between more parents would allow further improvement of stability of training, quality and diversity of generated images.

References

- [1] Yoshua Bengio, Grégoire Mesnil, Yann Dauphin, and Salah Rifai. Better mixing via deep representations. In *Proceedings of the 30th International Conference on Machine Learning, ICML 2013, Atlanta, GA, USA, 16-21 June 2013*, pages 552–560, 2013. URL <http://jmlr.org/proceedings/papers/v28/bengio13.html>.
- [2] Andrew Brock, Theodore Lim, James M. Ritchie, and Nick Weston. Neural photo editing with introspective adversarial networks. *CoRR*, abs/1609.07093, 2016. URL <http://arxiv.org/abs/1609.07093>.
- [3] Brian Cheung, Jesse A. Livezey, Arjun K. Bansal, and Bruno A. Olshausen. Discovering hidden factors of variation in deep networks. *CoRR*, abs/1412.6583, 2014. URL <http://arxiv.org/abs/1412.6583>.
- [4] Alexey Dosovitskiy, Jost Tobias Springenberg, and Thomas Brox. Learning to generate chairs with convolutional neural networks. *arXiv preprint arXiv:1411.5928*, 2014.
- [5] Jacob R. Gardner, Matt J. Kusner, Yixuan Li, Paul Upchurch, Kilian Q. Weinberger, and John E. Hopcroft. Deep manifold traversal: Changing labels with convolutional features. *CoRR*, abs/1511.06421, 2015. URL <http://arxiv.org/abs/1511.06421>.

- [6] Ian J. Goodfellow. NIPS 2016 tutorial: Generative adversarial networks. *CoRR*, abs/1701.00160, 2017. URL <http://arxiv.org/abs/1701.00160>.
- [7] Ian J. Goodfellow, Jean Pouget-Abadie, Mehdi Mirza, Bing Xu, David Warde-Farley, Sherjil Ozair, Aaron C. Courville, and Yoshua Bengio. Generative adversarial nets. In *Advances in Neural Information Processing Systems 27: Annual Conference on Neural Information Processing Systems 2014, December 8-13 2014, Montreal, Quebec, Canada*, pages 2672–2680, 2014. URL <http://papers.nips.cc/paper/5423-generative-adversarial-nets>.
- [8] Di He, Yingce Xia, Tao Qin, Liwei Wang, Nenghai Yu, Tie-Yan Liu, and Wei-Ying Ma. Dual learning for machine translation. In *Advances in Neural Information Processing Systems 29: Annual Conference on Neural Information Processing Systems 2016, December 5-10, 2016, Barcelona, Spain*, pages 820–828, 2016. URL <http://papers.nips.cc/paper/6469-dual-learning-for-machine-translation>.
- [9] Geoffrey E. Hinton, Alex Krizhevsky, and Sida D. Wang. Transforming auto-encoders. In *Artificial Neural Networks and Machine Learning - ICANN 2011 - 21st International Conference on Artificial Neural Networks, Espoo, Finland, June 14-17, 2011, Proceedings, Part I*, pages 44–51, 2011. doi: 10.1007/978-3-642-21735-7_6. URL http://dx.doi.org/10.1007/978-3-642-21735-7_6.
- [10] Sergey Ioffe and Christian Szegedy. Batch normalization: Accelerating deep network training by reducing internal covariate shift. *arXiv preprint arXiv:1502.03167*, 2015.
- [11] Taeksoo Kim, Moon-su Cha, Hyunsoo Kim, Jung Kwon Lee, and Jiwon Kim. Learning to discover cross-domain relations with generative adversarial networks. *CoRR*, abs/1703.05192, 2017. URL <http://arxiv.org/abs/1703.05192>.
- [12] Diederik P. Kingma, Shakir Mohamed, Danilo Jimenez Rezende, and Max Welling. Semi-supervised learning with deep generative models. In *Advances in Neural Information Processing Systems 27: Annual Conference on Neural Information Processing Systems 2014, December 8-13 2014, Montreal, Quebec, Canada*, pages 3581–3589, 2014. URL <http://papers.nips.cc/paper/5352-semi-supervised-learning-with-deep-generative-models>.
- [13] Tejas D. Kulkarni, William F. Whitney, Pushmeet Kohli, and Joshua B. Tenenbaum. Deep convolutional inverse graphics network. In *Advances in Neural Information Processing Systems 28: Annual Conference on Neural Information Processing Systems 2015, December 7-12, 2015, Montreal, Quebec, Canada*, pages 2539–2547, 2015. URL <http://papers.nips.cc/paper/5851-deep-convolutional-inverse-graphics-network>.
- [14] Ziwei Liu, Ping Luo, Shi Qiu, Xiaogang Wang, and Xiaoou Tang. Deepfashion: Powering robust clothes recognition and retrieval with rich annotations. In *2016 IEEE Conference on Computer Vision and Pattern Recognition, CVPR 2016, Las Vegas, NV, USA, June 27-30, 2016*, pages 1096–1104, 2016. doi: 10.1109/CVPR.2016.124. URL <http://dx.doi.org/10.1109/CVPR.2016.124>.

- [15] Christos Louizos, Kevin Swersky, Yujia Li, Max Welling, and Richard S. Zemel. The variational fair autoencoder. *CoRR*, abs/1511.00830, 2015. URL <http://arxiv.org/abs/1511.00830>.
- [16] Andrew L Maas, Awni Y Hannun, and Andrew Y Ng. Rectifier nonlinearities improve neural network acoustic models. In *Proc. ICML*, volume 30, 2013.
- [17] Stephen Moore and Richard Bowden. Multi-view pose and facial expression recognition. In *Proc. BMVC*, volume 2, 2010.
- [18] Guim Perarnau, Joost van de Weijer, Bogdan Raducanu, and Jose M. Álvarez. Invertible conditional gans for image editing. *CoRR*, abs/1611.06355, 2016. URL <http://arxiv.org/abs/1611.06355>.
- [19] Alec Radford, Luke Metz, and Soumith Chintala. Unsupervised representation learning with deep convolutional generative adversarial networks. *CoRR*, abs/1511.06434, 2015. URL <http://arxiv.org/abs/1511.06434>.
- [20] Scott E. Reed, Yi Zhang, Yuting Zhang, and Honglak Lee. Deep visual analogy-making. In *Advances in Neural Information Processing Systems 28: Annual Conference on Neural Information Processing Systems 2015, December 7-12, 2015, Montreal, Quebec, Canada*, pages 1252–1260, 2015. URL <http://papers.nips.cc/paper/5845-deep-visual-analogy-making>.
- [21] Jost Tobias Springenberg, Alexey Dosovitskiy, Thomas Brox, and Martin A. Riedmiller. Striving for simplicity: The all convolutional net. *CoRR*, abs/1412.6806, 2014. URL <http://arxiv.org/abs/1412.6806>.
- [22] Ilya Sutskever, James Martens, George E. Dahl, and Geoffrey E. Hinton. On the importance of initialization and momentum in deep learning. In *Proceedings of the 30th International Conference on Machine Learning, ICML 2013, Atlanta, GA, USA, 16-21 June 2013*, pages 1139–1147, 2013. URL <http://jmlr.org/proceedings/papers/v28/sutskever13.html>.
- [23] Paul Upchurch, Jacob R. Gardner, Kavita Bala, Robert Pless, Noah Snaveley, and Kilian Q. Weinberger. Deep feature interpolation for image content changes. *CoRR*, abs/1611.05507, 2016. URL <http://arxiv.org/abs/1611.05507>.
- [24] Xinchen Yan, Jimei Yang, Kihyuk Sohn, and Honglak Lee. Attribute2image: Conditional image generation from visual attributes. In *Computer Vision - ECCV 2016 - 14th European Conference, Amsterdam, The Netherlands, October 11-14, 2016, Proceedings, Part IV*, pages 776–791, 2016. doi: 10.1007/978-3-319-46493-0_47. URL http://dx.doi.org/10.1007/978-3-319-46493-0_47.
- [25] Shuo Yang, Ping Luo, Chen Change Loy, and Xiaoou Tang. WIDER FACE: A face detection benchmark. In *2016 IEEE Conference on Computer Vision and Pattern Recognition, CVPR 2016, Las Vegas, NV, USA, June 27-30, 2016*, pages 5525–5533, 2016. doi: 10.1109/CVPR.2016.596. URL <http://dx.doi.org/10.1109/CVPR.2016.596>.

- [26] Zili Yi, Hao Zhang, Ping Tan, and Minglun Gong. Dualgan: Unsupervised dual learning for image-to-image translation. *CoRR*, abs/1704.02510, 2017. URL <http://arxiv.org/abs/1704.02510>.
- [27] Weidong Yin, Yanwei Fu, Leonid Sigal, and Xiangyang Xue. Semi-latent gan: Learning to generate and modify facial images from attributes. *CoRR*, abs/1704.02166, 2017. URL <http://arxiv.org/abs/1704.02166>.
- [28] Jun-Yan Zhu, Philipp Krähenbühl, Eli Shechtman, and Alexei A. Efros. Generative visual manipulation on the natural image manifold. In *Computer Vision - ECCV 2016 - 14th European Conference, Amsterdam, The Netherlands, October 11-14, 2016, Proceedings, Part V*, pages 597–613, 2016. doi: 10.1007/978-3-319-46454-1_36. URL http://dx.doi.org/10.1007/978-3-319-46454-1_36.
- [29] Jun-Yan Zhu, Taesung Park, Phillip Isola, and Alexei A. Efros. Unpaired image-to-image translation using cycle-consistent adversarial networks. *CoRR*, abs/1703.10593, 2017. URL <http://arxiv.org/abs/1703.10593>.